Supporting Information

Design of Lipid-Protein Conjugates Using Amphiphilic Peptide Substrates of Microbial Transglutaminase.

Mari Takahara, [†,‡] *Rie Wakabayashi,* [†] *Kosuke Minamihata,* [†] *Masahiro Goto,* [†,§] *,Noriho Kamiya* [†,§,*]

† Department of Applied Chemistry, Graduate School of Engineering, Kyushu University, 744 Motooka, Fukuoka 819-0395, Japan.

‡ National Institute of Technology, Kitakyushu College, Department of Materials Science & Chemical Engineering, 5-20-1 Shii, Kokuraminamiku, Kitakyushu, Fukuoka, Japan.

§ Division of Biotechnology, Center for Future Chemistry, Kyushu University, 744 Motooka, Fukuoka 819-0395, Japan

*Corresponding Author

Tel: +81-(0)92-802-2807; Fax: +81-(0)92-802-2810; E-mail: kamiya.noriho.367@m.kyushu-u.ac.jp

Contents

1. Supplementary materials and methods

1-1. Fmoc solid-phase peptide synthesis of C_{14}-X-MRHKGS-NH_2

All the peptides (C_{14}-X-MRHKGS-NH_2, Figure S1) were manually prepared by Fmoc solid-phase peptide synthesis. Rink Amide AM resin LL (0.05 or 0.1 mmol) loaded on a PD-10 empty column (GE healthcare) was pre-swollen in DCM for 60 min. The swollen resin was coupled with Fmoc-protected amino acids after removal of N-terminal Fmoc protecting group. In coupling reactions, Fmoc-protected amino acids (3.0 equiv. to the loaded resin) were first activated in a coupling cocktail containing HBTU (3.0 equiv.), HOBt (3.0 equiv.), and DIPEA (6.0 equiv.) in DMF, and activated amino acids were subjected to the resin for a 60-min coupling. The completion of the reaction was confirmed by a nynhydrin test. The removal of N-terminal Fmoc protection groups on a resin was proceeded by the treatment of 20% (v/v) piperidine in DMF for 10 min. After proceeding the attachment of every peptidyl components, the resin-bound NH_2-X-MRHKGS was subjected to mylistic acid (C_{14}-OH, 6.0 equiv.) in a coupling cocktail for 60 min and C_{14}-modification was confirmed by a nynhydrin test. The deprotection and cleavage of C_{14}-modified peptides from a resin was carried out soaking the resin in a solution of TFA/H_2O/TIS/EDT (94/2.5/1.0/2.5) for 120 min. The crude lipid-fused peptides were obtained after precipitation with cold diethyl ether and dried under room temperature.

The crude peptides were dissolved in a ACN/water (30/70, 0.1% TFA) and injected into a SunFireC_{18} column 19×50 mm (Waters Corporation, Milford, MA) for RP-HPLC purification. The RP-HPLC condition is following: flow rate; 9.0 mL/min, detection wavelength; 220 nm, mobile phase; ACN/water (0.1% TFA) = 30/70→50/50 (15 min). The collected fractions were lyophilized. All the peptides were dissolved in water just before use and stored at 4 °C.

The synthesized lipid-fused peptides were identified by MALDI-TOF-MS analysis. Mass spectra of peptides spotted on a CHCA matrix were obtained with a Bruker Autoflex-III MALDI-TOF MS (Bruker, Billerica, MA) in a positive ion detection mode. Theoretical masses were calculated using the program ChemDraw (CambridgeSoft Corporation, Waltham, MA).

The purity of peptides was estimated with RP-HPLC analysis. In a RP-HPLC (GL Science, Tokyo, Japan), 0.5 mg/mL C_{14}-X-MRHKGS in a ACN/water (30/70, 0.1% TFA) were injected into a Inertsil ODS-3 (4.6× 250 mm) column (GL Science) with a following analysis condition: flow rate; 1.0 mL/min, detection wavelength; 220 nm, mobile phase; ACN/water (0.1% TFA) = 30/70→60/40 (30 min). The purity was determined by the integration of C_{14}-X-MRHKGS and impurities.

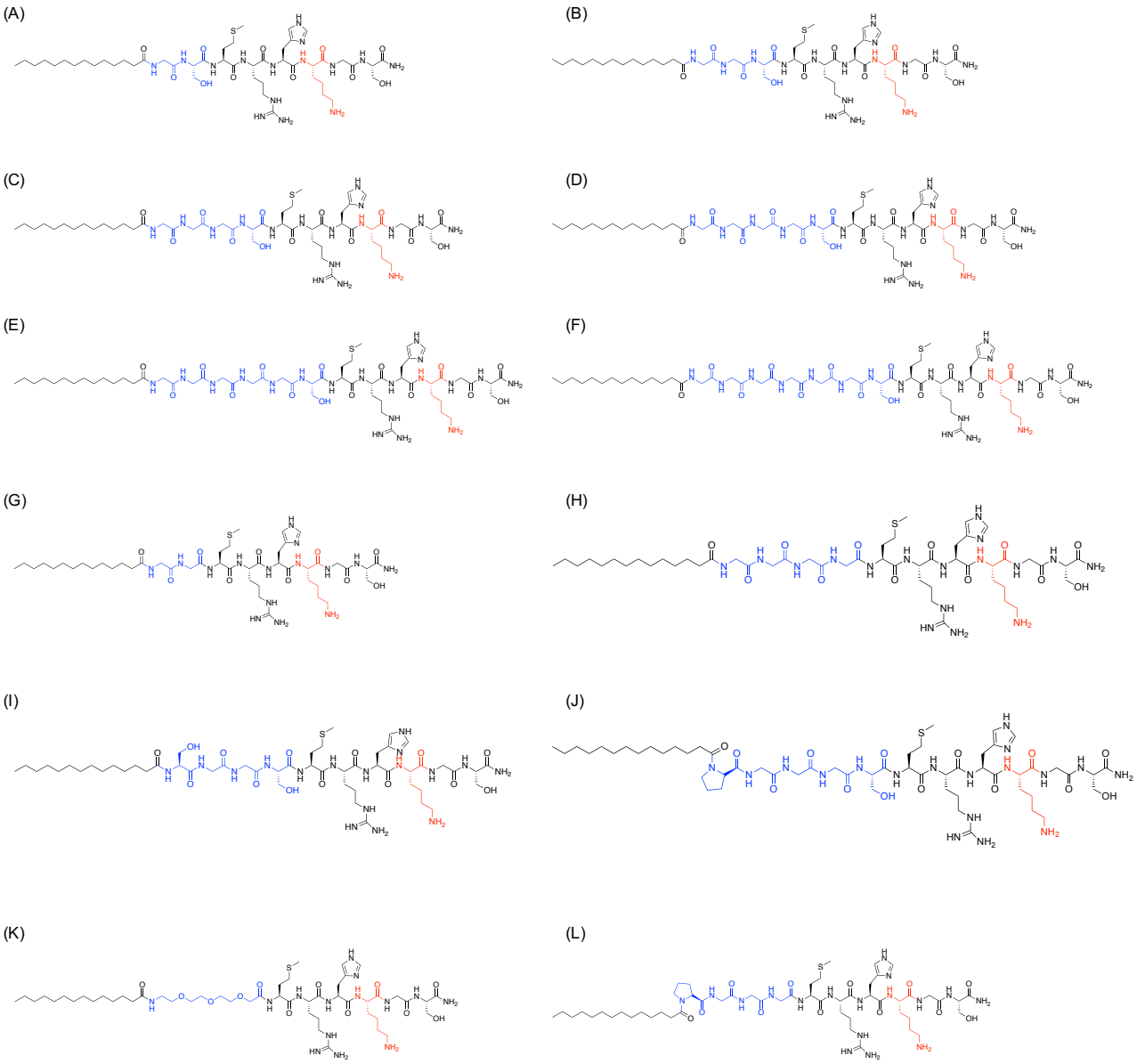

Figure S1. Chemical structures of synthesized lipid-fused peptides. (A) C_{14}-GS-MRHKGS, (B) C_{14}-G_2S-MRHKGS, (C) C_{14}-G_3S-MRHKGS, (D) C_{14}-G_4S-MRHKGS, (E) C_{14}-G_5S-MRHKGS, (F) C_{14}-G_6S-MRHKGS, (G) C_{14}-G_2-MRHKGS, (H) C_{14}-G_4-MRHKGS, (I) C_{14}-SG_2S-MRHKGS, (J) C_{14}-PG_3S-MRHKGS, (K) C_{14}-PEG-MRHKGS, (L) C_{14}-PG_3-MRHKGS.

1-2. Purification of C_{14}-G_5S-EGFP after MTG reaction

In order to increase the conversion rate of MTG reaction, the surfactant *n*-dodecyl maltoside that can migrate the aggregation of C_{14}-G_5S-MRHKGS was added in MTG reaction solution containing 10 μM LQ-EGFP, 50 μM C_{14}-G_5S-MRHKGS, 0.1 U/mL MTG and 1% (w/v) *n*-dodecyl maltoside (Sigma-Aldrich, St. Lois, MO) in 10 mM Tris-HCl (pH 8.0) buffer. The reaction solution was incubated for 60 min at 37 °C, followed by addition of 1 mM *N*-ethylmaleimide (Wako Pure Chemical Industries, Osaka, Japan) to terminate the reaction.

The MTG reaction product was purified using Ni-NTA slurry according to the manufacture's protocol[1,2] and desalted through PD SpinTrap G-25 (GE healthcare) using PBS as an elution buffer. The concentration of purified and buffer-exchanged C_{14}-G_5S-EGFP was determined by UV-Vis measurement at 488 nm using a molar extinction coefficient of 55000 $M^{-1}cm^{-1}$. The purity of C_{14}-G_5S-EGFP was confirmed by RP-HPLC as following: 20 μL injection of 5 μM C_{14}-G_5S-EGFP in PBS/ACN (50/50, 0.1% TFA), column; Inertsil ODS-3 (4.6×250 mm), flow rate; 1.0 mL/min, detection wavelength; 280 nm, mobile phase; ACN/water (0.1% TFA) = 20/80→0/100 (40 min).

2. Supplementary results

2-1. MALDI-TOF-MS results and RP-HPLC analysis of C_{14}-X-MRHKGS-NH_2

All the obtained peptides were colorless solids. Yields were not determined. The identity and purity of synthesized peptides were confirmed by MALDI-TOF-MS and RP-HPLC. The results shown in Figures S2-S4 were summarized as following:

(A) Myr-Met-Arg-His-Lys-Gly-Ser-NH_2 (C_{14}-MRHKGS)
m/z: calculated for $C_{42}H_{78}N_{13}O_8S$ ($[M+H]^+$) 924.6, found 924.3, purity: 99.0%

(B) Myr-Gly-Ser-Met-Arg-His-Lys-Gly-Ser-NH_2 (C_{14}-GS-MRHKGS)
m/z: calculated for $C_{47}H_{86}N_{15}O_{11}S$ ($[M+H]^+$) 1068.6, found 1067.8, purity: 99.9%

(C) Myr-Gly-Gly-Ser-Met-Arg-His-Lys-Gly-Ser-NH_2 (C_{14}-G_2S-MRHKGS)
m/z: calculated for $C_{49}H_{89}N_{16}O_{12}S$ ($[M+H]^+$) 1125.6, found 1124.6, purity: 99.9%

(D) Myr-Gly-Gly-Gly-Ser-Met-Arg-His-Lys-Gly-Ser-NH_2 (C_{14}-G_3S-MRHKGS)
m/z: calculated for $C_{51}H_{92}N_{17}O_{13}S$ ($[M+H]^+$) 1182.6, found 1182.5, purity: 99.9%

(E) Myr-Gly-Gly-Gly-Gly-Ser-Met-Arg-His-Lys-Gly-Ser-NH_2 (C_{14}-G_4S-MRHKGS)
m/z: calculated for $C_{53}H_{95}N_{18}O_{14}S$ ($[M+H]^+$) 1238.6, found 1238.1, purity: 99.0%

(F) Myr-Gly-Gly-Gly-Gly-Gly-Ser-Met-Arg-His-Lys-Gly-Ser-NH_2 (C_{14}-G_5S-MRHKGS)
m/z: calculated for $C_{55}H_{98}N_{19}O_{15}S$ ($[M+H]^+$) 1296.7, found 1296.8, purity: 97.0%

(G) Myr-Gly-Gly-Gly-Gly-Gly-Gly-Ser-Met-Arg-His-Lys-Gly-Ser-NH_2 (C_{14}-G_6S-MRHKGS)
m/z: calculated for $C_{57}H_{101}N_{20}O_{16}S$ ($[M+H]^+$) 1354.6, found 1354.6, purity: 97.8%

(H) Myr-Gly-Gly-Met-Arg-His-Lys-Gly-Ser-NH_2 (C_{14}-G_2-MRHKGS)
m/z: calculated for $C_{46}H_{84}N_{15}O_{10}S$ ($[M+H]^+$) 1038.3, found 1037.9, purity: 99.0%

(I) Myr-Gly-Gly-Gly-Gly-Met-Arg-His-Lys-Gly-Ser-NH_2 (C_{14}-G_4-MRHKGS)
m/z: calculated for $C_{50}H_{90}N_{17}O_{12}S$ ($[M+H]^+$) 1153.4, found 1153.8, purity:99.8%

(J) Myr-Ser-Gly-Gly-Ser-Met-Arg-His-Lys-Gly-Ser-NH_2 (C_{14}-SG_2S-MRHKGS)
m/z: calculated for $C_{53}H_{95}N_{18}O_{14}S$ ($[M+H]^+$) 1212.6, found 1212.5, purity: 88.0%

(K) Myr-Pro-Gly-Gly-Gly-Ser-Met-Arg-His-Lys-Gly-Ser-NH_2 (C_{14}-PG_3S-MRHKGS)
m/z: calculated for $C_{56}H_{99}N_{18}O_{14}S$ ($[M+H]^+$) 1280.6, found 1281.9, purity: 100%

(L) Myr-PEG-Met-Arg-His-Lys-Gly-Ser-NH_2 (C_{14}-PEG-MRHKGS)
m/z: calculated for $C_{50}H_{93}N_{14}O_{12}S$ ($[M+H]^+$) 1113.6, found 1113.4, purity: 94.0%

(M) Myr-Pro-Gly-Gly-Gly-Met-Arg-His-Lys-Gly-Ser-NH_2 (C_{14}-PG_3-MRHKGS)
m/z: calculated for $C_{53}H_{94}N_{17}O_{12}S$ ($[M+H]^+$) 1192.6, found 1192.3, purity: 90.0%

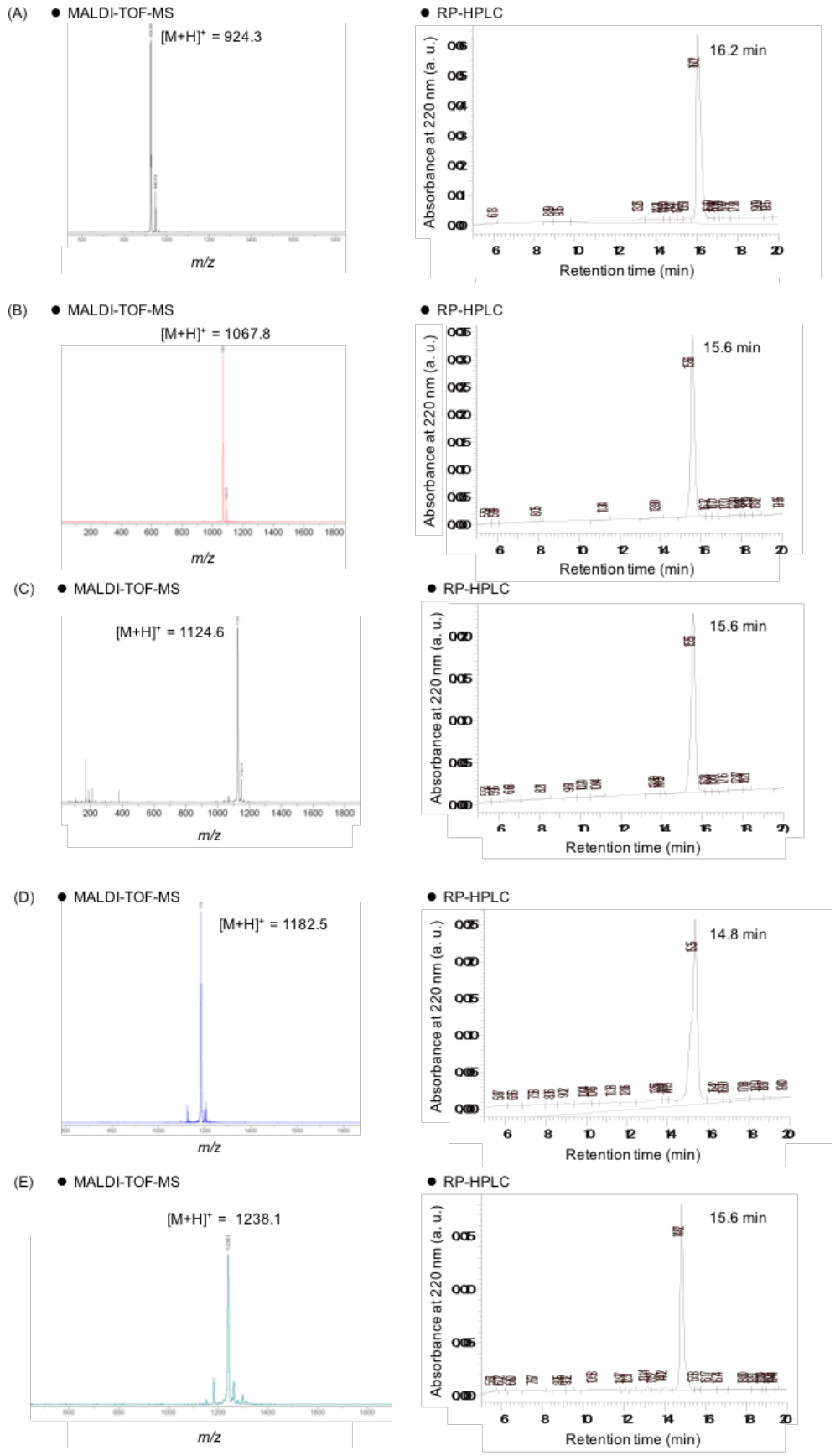

Figure S2. MALDI-TOF-MS and RP-HPLC results of (A) C_{14}-MRHKGS, (B) C_{14}-GS-MRHKGS, (C) C_{14}-G_2S-MRHKGS, (D) C_{14}-G_3S-MRHKGS, (E) C_{14}-G_4S-MRHKGS.

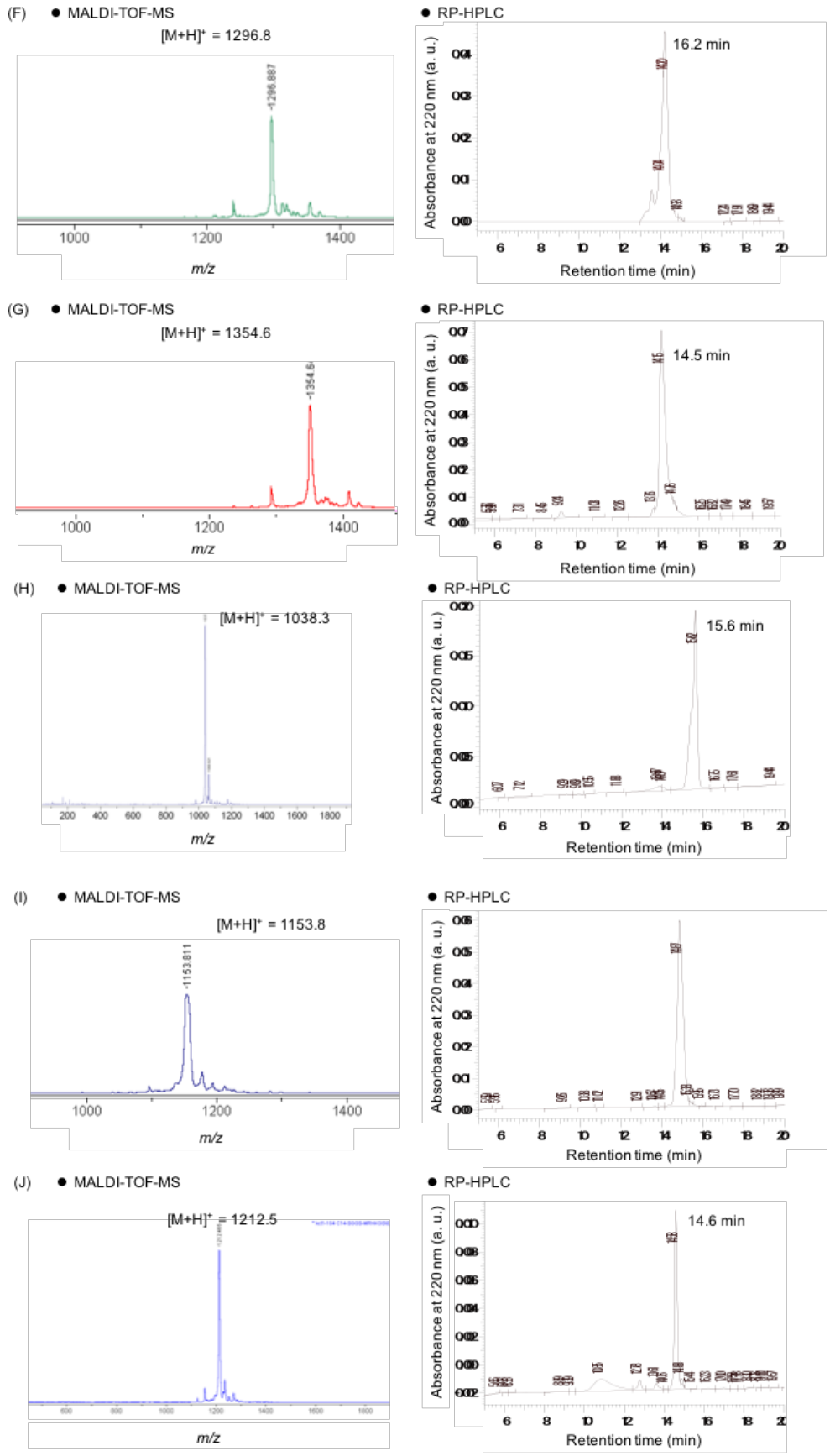

Figure S3. MALDI-TOF-MS and RP-HPLC results of (F) C_{14}-G_5S-MRHKGS, (G) C_{14}-G_6S-MRHKGS, (H) C_{14}-G_2-MRHKGS, (I) C_{14}-G_4-MRHKGS, (J) C_{14}-SG_2S-MRHKGS.

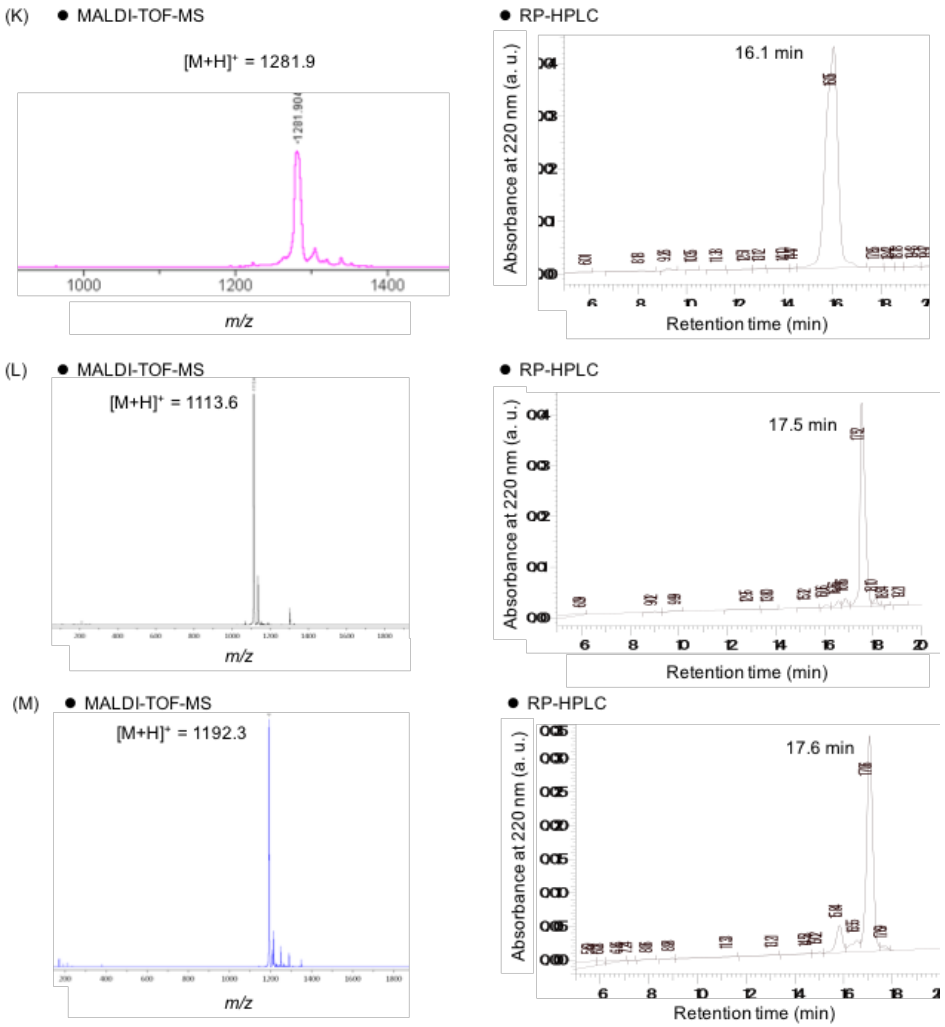

Figure S4. MALDI-TOF-MS and RP-HPLC results of (K) C_{14}-PG_3S-MRHKGS, (L) C_{14}-PEG-MRHKGS, (M) C_{14}-PG_3-MRHKGS.

2-2. Solubility comparison of C_{14}-G_3S-MRHKGS-NH_2 and C_{14}-G_3S-LLQG-OH

The lipid-fused peptides, C_{14}-G_3S-MRHKGS (Figure 1A) or C_{14}-G_3S-LLQG (Figure S5A), were dissolved in PBS to compare their solubility. C_{14}-G_3S-MRHKGS dissolved in PBS up to 100 μM (transparent solution, Figure S5B, left), while C_{14}-G_3S-LLQG become clouded at 100 μM (Figure S5B, right). Considering that both peptides have the same C_{14}-moiety, difference of solubility toward PBS derived from peptidyl moiety, suggesting that hydrophilic and basic amino acids in MRHKGS improved the poor solubility of the hydrophobic C_{14}-G_3S-LLQG.

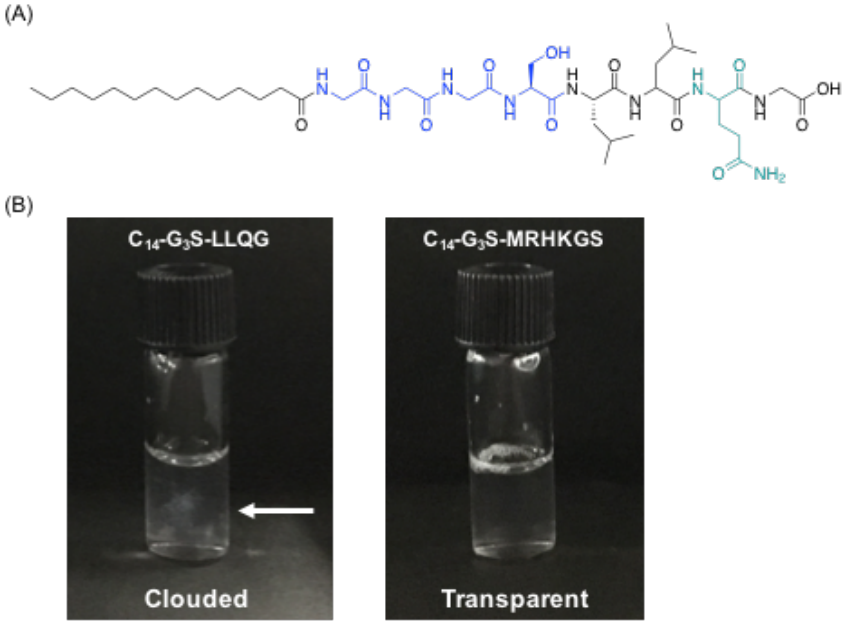

Figure S5. (A) Chemical structure of C_{14}-G_3S-LLQG. (B) Lipid-fused peptides (100 μM) in PBS. (left) C_{14}-G_3S-LLQG, (right) C_{14}-G_3S-MRHKGS.

2-3. MALDI-TOF-MS results of MTG reaction products

One microliter of MTG reaction products (10 μM LQ-EGFP, 50 μM C_{14}-X-MRHKGS, 0.1 U/mL MTG for 30 min, stopped by 1 mM NEM) were spotted on a CHCA matrix and analyzed by MALDI-TOF-MS measurement. The identification of reaction products was confirmed by the theoretical increase of mass (Δ_{theo}) from the unreacted LQ-EGFP. The found mass difference (Δ_{found}) was the subtraction of MTG reaction products from the unreacted LQ-EGFP.

All the obtained data summarized below. The Δ_{found} matches Δ_{theo} within ±50, confirming attachment of single C_{14}-G_nS-MRHKGS on a LQ-EGFP.

(A) C_{14}-EGFP (LQ-EGFP attached with C_{14}-MRHKGS)
Δ_{theo} = 908.52
Δ_{found} = 897.33

(B) C_{14}-GS-EGFP (LQ-EGFP attached with C_{14}-GS-MRHKGS)
Δ_{theo} = 1037.6
Δ_{found} = 1037.7

(C) C_{14}-G_2S-EGFP (LQ-EGFP attached with C_{14}-G_2S-MRHKGS)
Δ_{theo} = 1094.7
Δ_{found} = 1047.6

(D) C_{14}-G_3S-EGFP (LQ-EGFP attached with C_{14}-G_3S-MRHKGS)
Δ_{theo} = 1151.6
Δ_{found} = 1137.3

(E) C_{14}-G_4S-EGFP (LQ-EGFP attached with C_{14}-G_4S-MRHKGS)
Δ_{theo} = 1212.6
Δ_{found} = 1212.2

(F) C_{14}-G_5S-EGFP (LQ-EGFP attached with C_{14}-G_5S-MRHKGS)
Δ_{theo} = 1278.7
Δ_{found} = 1275.9

(G) C_{14}-G_6S-EGFP (LQ-EGFP attached with C_{14}-G_6S-MRHKGS)
Δ_{theo} = 1336.6
Δ_{found} = 1326.8

(H) C_{14}-G_2-EGFP (LQ-EGFP attached with C_{14}-G_2-MRHKGS)
Δ_{theo} = 1007.6
Δ_{found} = 989.27

(I) C_{14}-G_4-EGFP (LQ-EGFP attached with C_{14}-G_4-MRHKGS)
Δ_{theo} = 1135.4
Δ_{found} = 1121.5

(J) C_{14}-SG_2S-EGFP (LQ-EGFP attached with C_{14}-SG_2S-MRHKGS)

Δ_{theo} = 1193.6

Δ_{found} = 1206.9

(K) C_{14}-PG_3S-EGFP (LQ-EGFP attached with C_{14}-PG_3S-MRHKGS)

Δ_{theo} = 1262.6

Δ_{found} = 1259.9

(L) C_{14}-PEG-EGFP (LQ-EGFP attached with C_{14}-PEG-MRHKGS)

Δ_{theo} = 1096.7

Δ_{found} = 1095.4

(M) C_{14}-PG_3-EGFP (LQ-EGFP attached with C_{14}-PG_3-MRHKGS)

Δ_{theo} = 1174.7

Δ_{found} = 1164.5

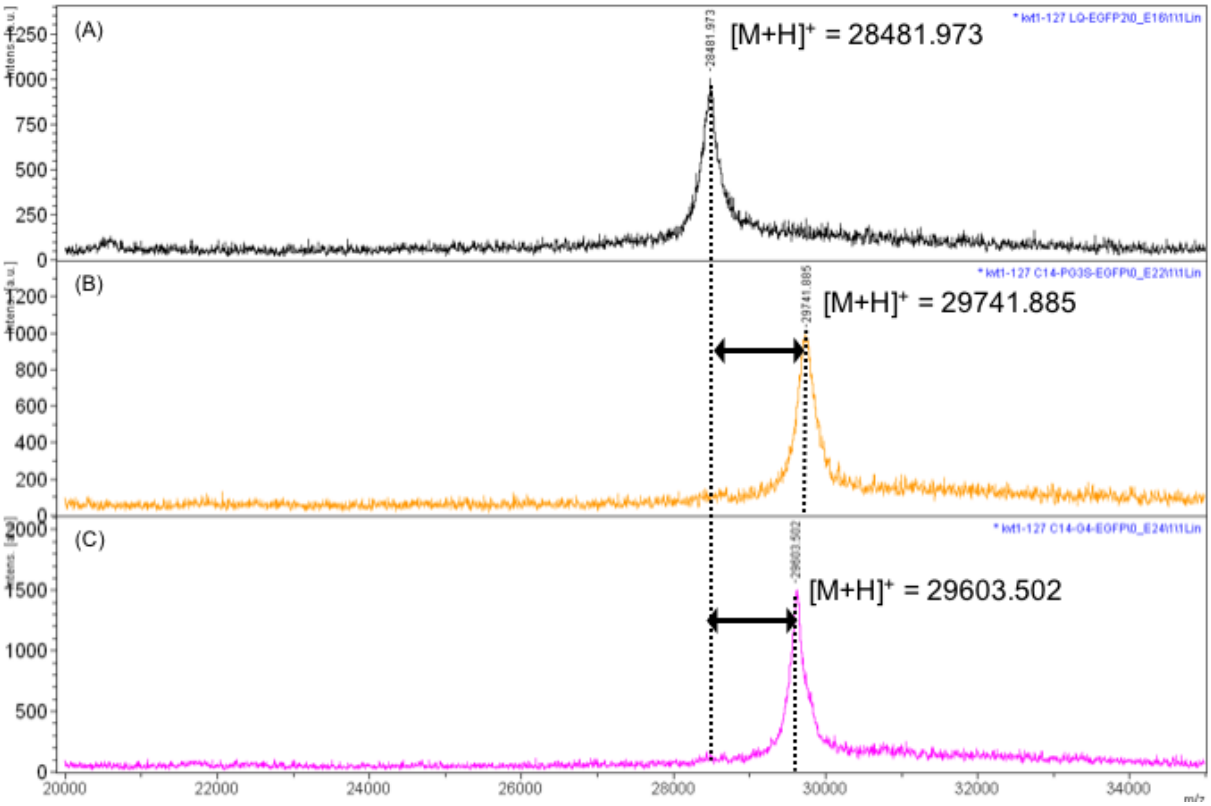

Figure S6. MALDI-TOF-MS analysis of MTG reaction product. (A) LQ-EGFP alone, (B) C_{14}-PG_3S-EGFP, (C) C_{14}-G_4-EGFP.

2-4. Fluorescence spectra measurement

The fluorescence spectra of FQ-EGFP, mixture of FQ-EGFP and C_{14}-(G_3S)-MRHKGS without MTG, MTG reaction solution containing FQ-EGFP and C_{14}-(G_3S)-MRHKGS with MTG were measured using LS-55 (Perkin Elmer, Waltham, MA). The sample PBS solutions composed of FQ-EGFP (10 μM), C_{14}-(G_3S)-MRHKGS (50 μM), and MTG (0.1 U/mL) were incubated for 30 min at 37 °C, subsequently mixed with NEM (1 mM). In the presence of MTG, cross-linking reaction between yielded C_{14}-(G_3S)-EGFP. The incubated samples were diluted to 100 nM FQ-EGFP in PBS, and their fluorescence spectra were recorded following conditions: 1 mm quart cell, excitation wavelength; 488 nm, emission wavelength; 500 to 600 nm, slit; 5 nm, scanning rate; 100 nm/min. The blank spectrum (PBS) subtraction was performed for all the obtained sample spectra.

The fluorescence spectra shapes of C_{14}-(G_3S)-EGFP after MTG reaction remained unchanged from the unreacted FQ-EGFP alone although decreased maximum intensity. Considering that C_{14}-(G_3S)-EGFP could aggregate by the attached lipid, quenching occurred at the high local concertation. The increased intensity of mixture of FQ-EGFP and C_{14}-(G_3S)-MRHKGS might be caused by the dispersed FQ-EGFP in the presence of C_{14}-(G_3S)-MRHKGS that functions as surfactant below CMC.

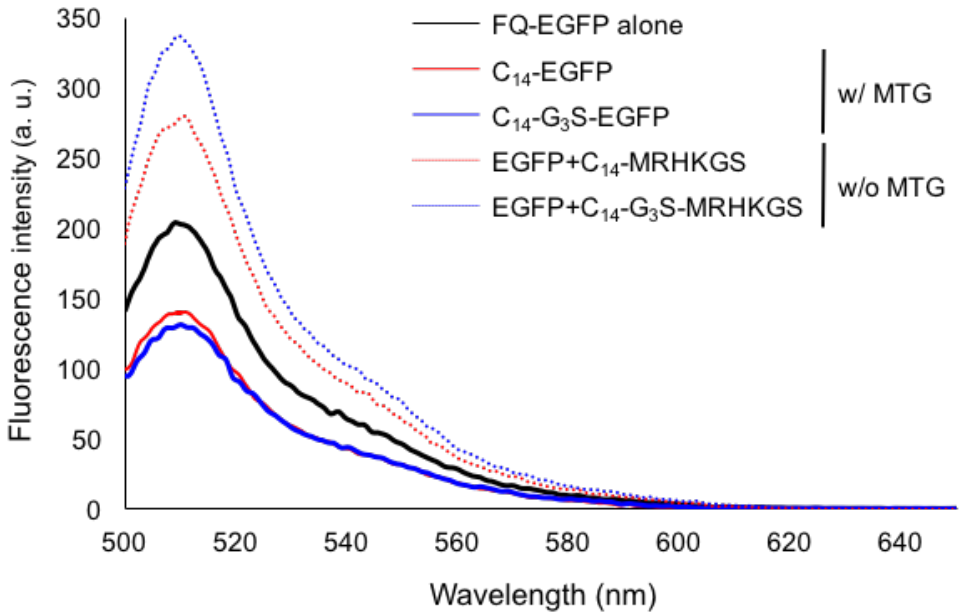

Figure S7. Fluorescence spectra of FQ-EGFP, FQ-EGFP and C_{14}-(G_3S)-MRHKGS in the presence or absence of MTG. In the presence of MTG, conjugated C_{14}-(G_3S)-EGFP was contained in the samples.

2-5. Circular dichroism (CD) measurement

C_{14}-X-MRHKGS (50 μM) were incubated in PBS prior to a measurement for 15 min and CD spectra of peptides were measured. All spectra were background-subtracted using PBS as a blank.

The obtained CD spectra were shown in Figure S8. C_{14}-MRHKGS, C_{14}-PG_3S-MRHKGS, C_{14}-G_4-MRHKGS were CD silent, while positive around 205 nm and negative around 220 nm of C_{14}-G_nS-MRHKGS (n = 3-5) showed β-sheet formation. The negative peak around 205 nm of C_{14}-G_6S-MRHKGS indicates the random coil formation. Thus, secondary structures of 50 μM C_{14}-G_nS-MRHKGS (n = 3-6) in PBS were the same as those at 100 μM.

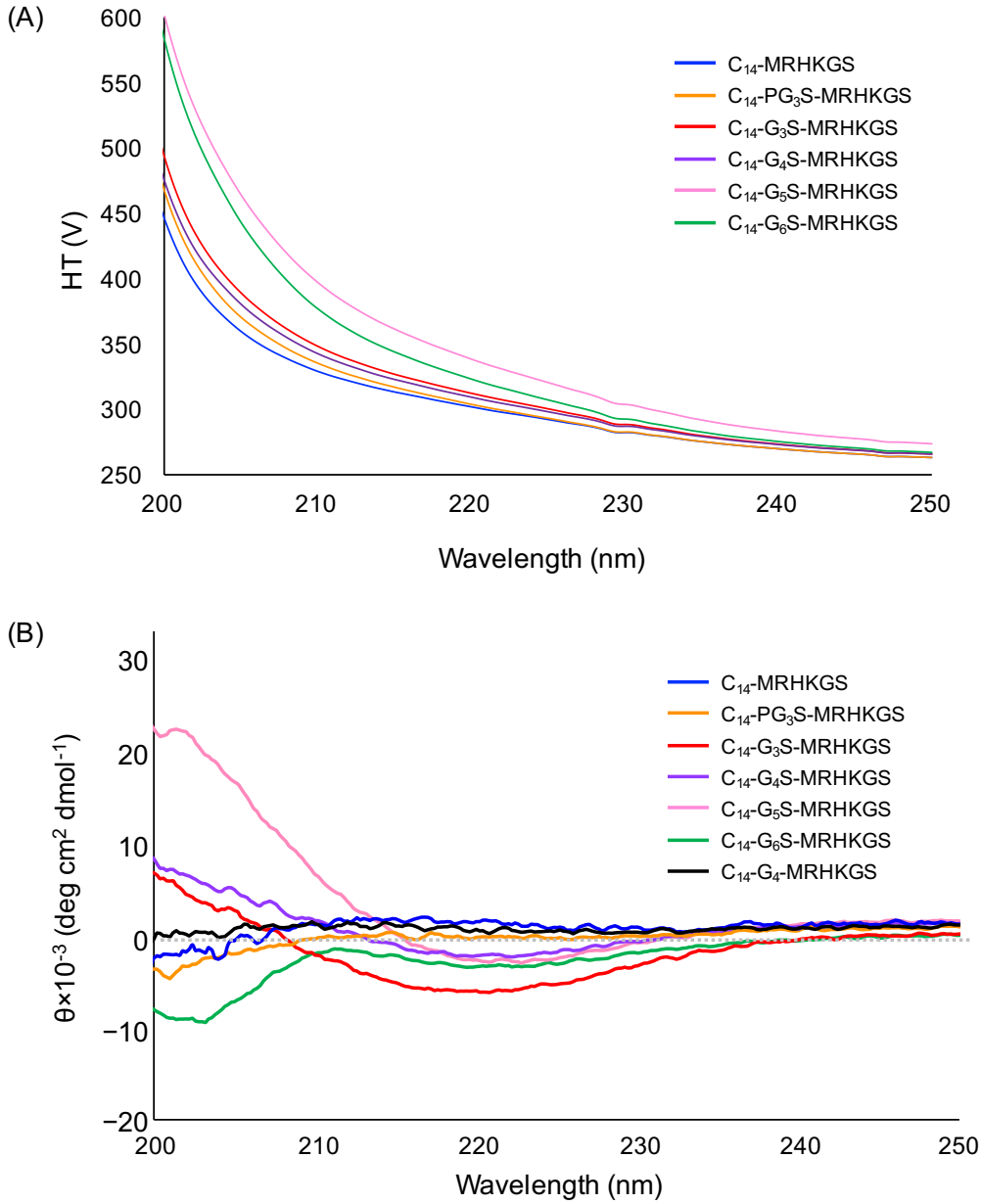

Figure S8. (A) Photomultiplier voltage (HT) level during CD measurement of 100 μM C_{14}-X-MRHKGS (Figure 3). (B) CD spectra of C_{14}-X-MRHKGS (50 μM) in PBS. C_{14}-MRHKGS (blue), C_{14}-PG_3S-MRHKGS (orange), C_{14}-G_3S-MRHKGS (red), C_{14}-G_4S-MRHKGS (purple), C_{14}-G_5S-MRHKGS (pink), C_{14}-G_6S-MRHKGS (green), C_{14}-G_4-MRHKGS (black).

Table S1. Estimated secondary structure content (%) of C_{14}-G_nS-MRHKGS peptides (*n* = 5 or 6).

	α-Helix	β-sheet	Turn	Others
C_{14}-G_5S-MRHKGS	4.80	76.4	7.20	11.7
C_{14}-G_6S-MRHKGS	0.00	24.8	15.8	59.4

2-6. MTG reaction of C_{14}-X-MRHKGS and LQ-EGFP

The MTG reaction between LQ-EGFP and C_{14}-X-MRHKGS was performed in the following condition: 10 μM LQ-EGFP, 50 μM C_{14}-X-MRHKGS, 0.1 U/mL MTG for 60 min for time-course analysis, and 10 μM LQ-EGFP, 10-200 μM C_{14}-X-MRHKGS, 0.1 U/mL MTG for 30 min for substrate ratio effect. The MTG reaction product was analyzed by RP-HPLC and evaluated as conversion rate of LQ-EGFP. RP-HPLC conditions were following: 20 μL injection of 5 μM C_{14}-X-EGFP in PBS/ACN (50/50, 0.1% TFA), column; Inertsil ODS-3 (4.6×250 mm), flow rate; 1.0 mL/min, detection wavelength; 280 nm, mobile phase; ACN/water (0.1% TFA) = 20/80→0/100 (40 min).

The time-course analysis was shown in Figure S9. Almost all the MTG reactions of C_{14}-X-MRHKGS and LQ-EGFP were saturated at 10-15 min except for the case of C_{14}-G_3S-MRHKGS (X = G_3S) was saturated at 30 min. The slight decreased conversion rate after 30 min indicated that the competitive hydrolysis reaction of MTG catalysis occurred, resulting in lowering the conversion rate. In the case of X = G_3S or G_5S, the conversion rate was approximately 80% at maximum while others showed over 90%. Although some peptides (X = SG_2S, G_5S) showed slight decreased conversion rate after 30 min, we selected C_{14}-G_3S-MRHKGS as a standard substrate, thus 30 min was selected as saturated reaction time.

In addition, the substrate ratio of [K]/[Q] (= [C_{14}-X-MRHKGS]/[LQ-EGFP]) effect on MTG reaction was shown in Figure S10. The conversion rate increased in accordance with [K]/[Q] ratio, with the maximum conversion rate at [K]/[Q] = 5 for X = GS, G_2S, G_2, PEG, PG_3, G_4, PG_3S, G_5S, G_6S, [K]/[Q] = 10 for X = G_4S, [K]/[Q] = 20 for X = G_3S, SG_2S. The decreased conversion rate at [K]/[Q] = 20 for X = G_5S, G_6S suggest that high concentration of lipid-fused peptides (X = G_5S, G_6S) caused aggregation, leading to inhibit MTG recognition and accompanied lower conversion rate than that at [K]/[Q] = 5. Considering that lowest CC_{50} of C_{14}- MRHKGS was 73.8 μM, where concentration of C_{14}-MRHKGS is over CC_{50} in the case of [K]/[Q] ≧10 ([C_{14}-MRHKGS] ≧ 100 μM), C_{14}-X-MRHKGS at [K]/[Q] = 5 is biocompatible and efficient reaction condition. Thus, we selected 30 min and [K]/[Q] = 5 as an optimized condition of MTG reaction between LQ-EGFP and C_{14}-X-MRHKGS.

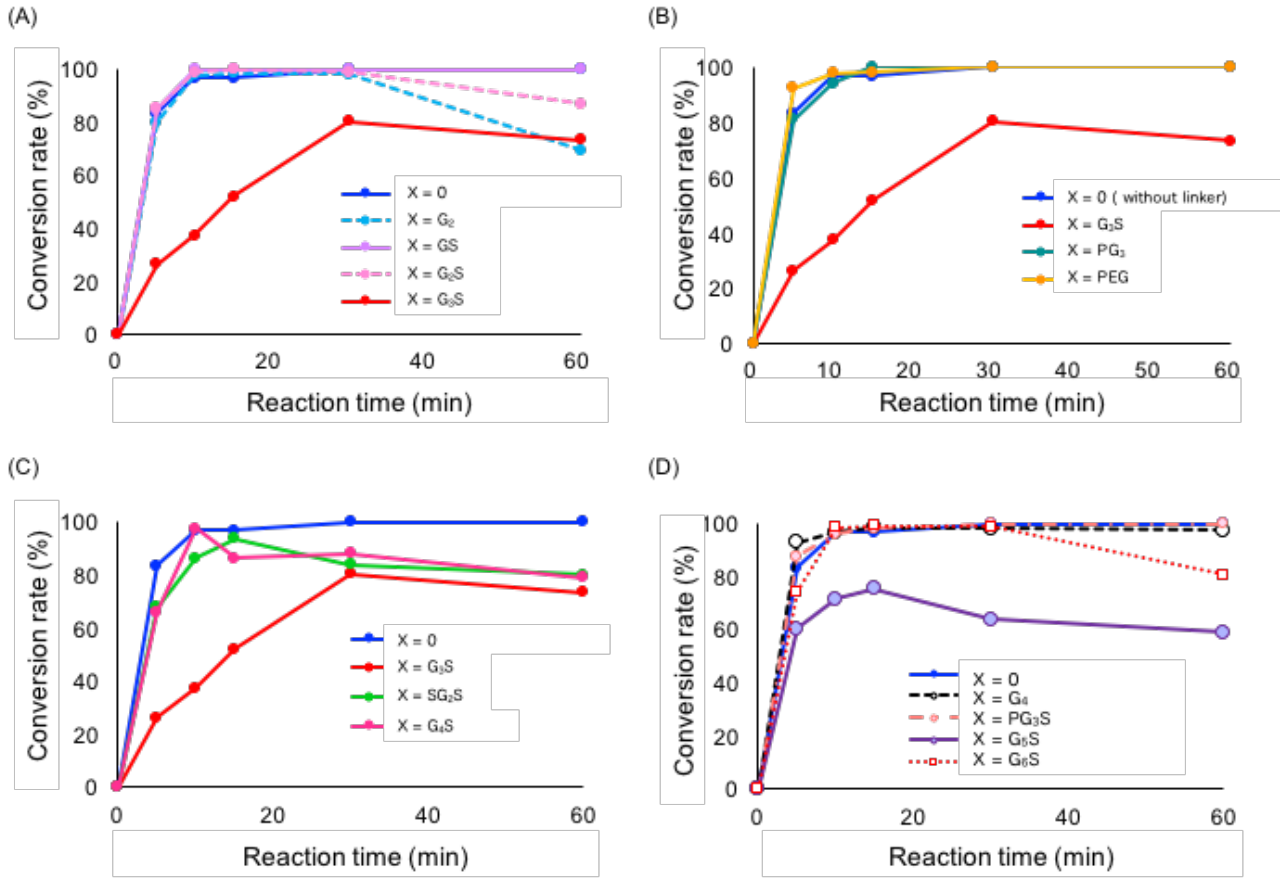

Figure S9. Time-course analysis of MTG reaction between LQ-EGFP and C_{14}-X-MRHKGS. (A) C_{14}-MRHKGS, C_{14}-G_nS-MRHKGS (n = 1-3), C_{14}-G_2-MRHKGS, (B) C_{14}-PEG-MRHKGS, C_{14}-PG_3-MRHKGS, (C) C_{14}-SG_2S-MRHKGS, C_{14}-G_4S-MRHKGS, (D) C_{14}-PG_3S-MRHKGS, C_{14}-G_4-MRHKGS, C_{14}-G_nS-MRHKGS (n = 5, 6). C_{14}-MRHKGS or C_{14}-G_3S-MRHKGS were inserted for standard.

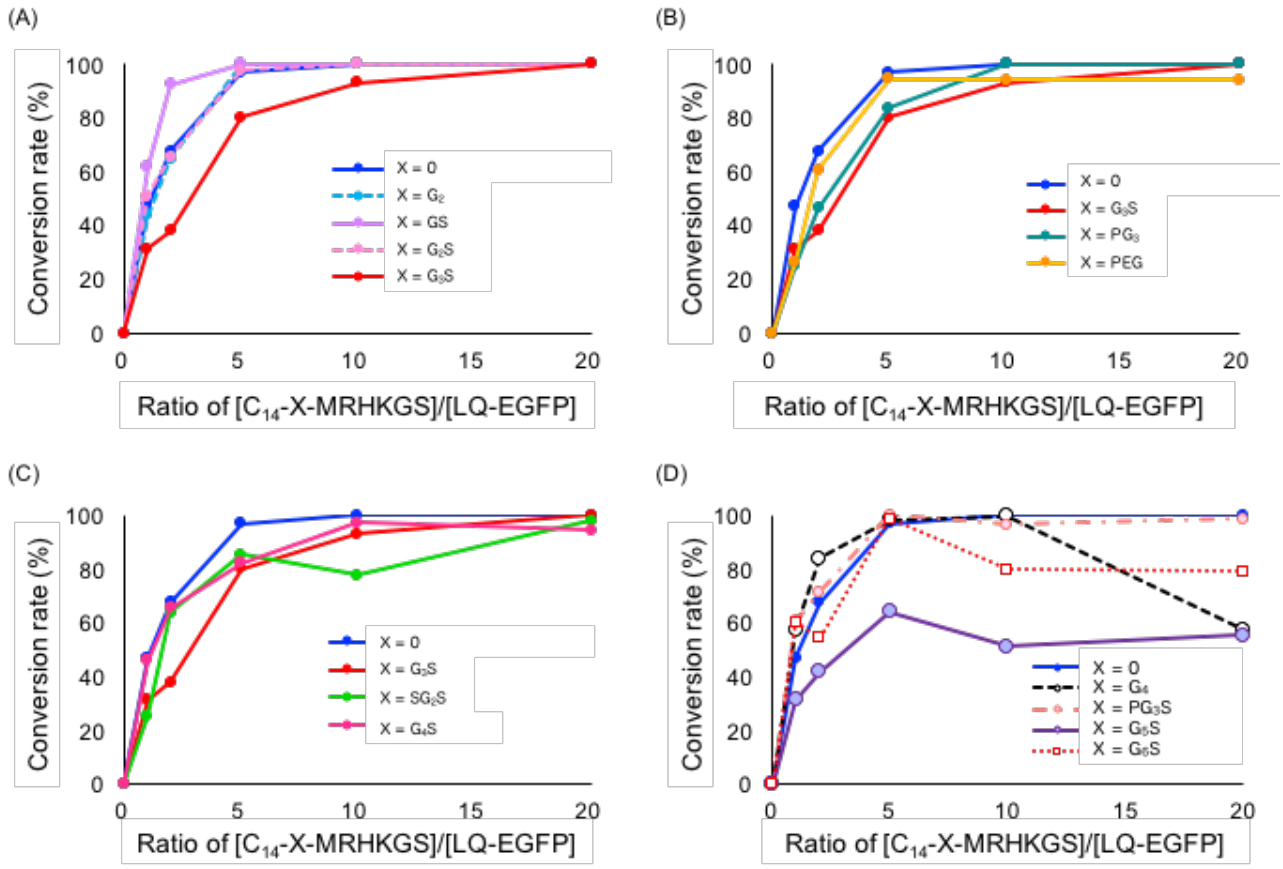

Figure S10. Effect of substrate ratio on MTG reaction between LQ-EGFP and C_{14}-X-MRHKGS. (A) C_{14}-MRHKGS, C_{14}-G_nS-MRHKGS (n = 1-3), C_{14}-G_2-MRHKGS, (B) C_{14}-PEG-MRHKGS, C_{14}-PG_3-MRHKGS, (C) C_{14}-SG_2S-MRHKGS, C_{14}-G_4S-MRHKGS, (D) C_{14}-PG_3S-MRHKGS, C_{14}-G_4-MRHKGS, C_{14}-G_nS-MRHKGS (n = 5, 6). C_{14}-MRHKGS or C_{14}-G_3S-MRHKGS were inserted for standard.

2-7. Critical micelle concentration (CMC) measurement

The CMC of each C_{14}-X-MRHKGS was measured by pyrene 1:3 ratio method.[3] Two microliter of pyrene (100 μM) in THF was spotted in a glass microtube, and THF was dried at room temperature. C_{14}-X-MRHKGS (100 μL, 0-2.5 mM) in PBS was incubated in the tube containing pyrene for 60 min at 35 °C with 30 rpm. The incubated peptides (50 μL) containing pyrene with three parallel preparation was subjected to the 96-well black half area plate (Grainer Bio One, Kremsmünster, Australia), and fluorescence measurement using LS-55 was carried out following conditions: an excitation wavelength; 335 nm, emission wavelength; 373 and 384 nm (whose intensities are abbreviated as I_{373} and I_{384}, respectively), slit; 15 nm. The ratio I_{373}/I_{384} (pyrene 1:3 ratio) versus concentration plot was generated followed by CMC determination. All the CMC values were shown in Table 1.

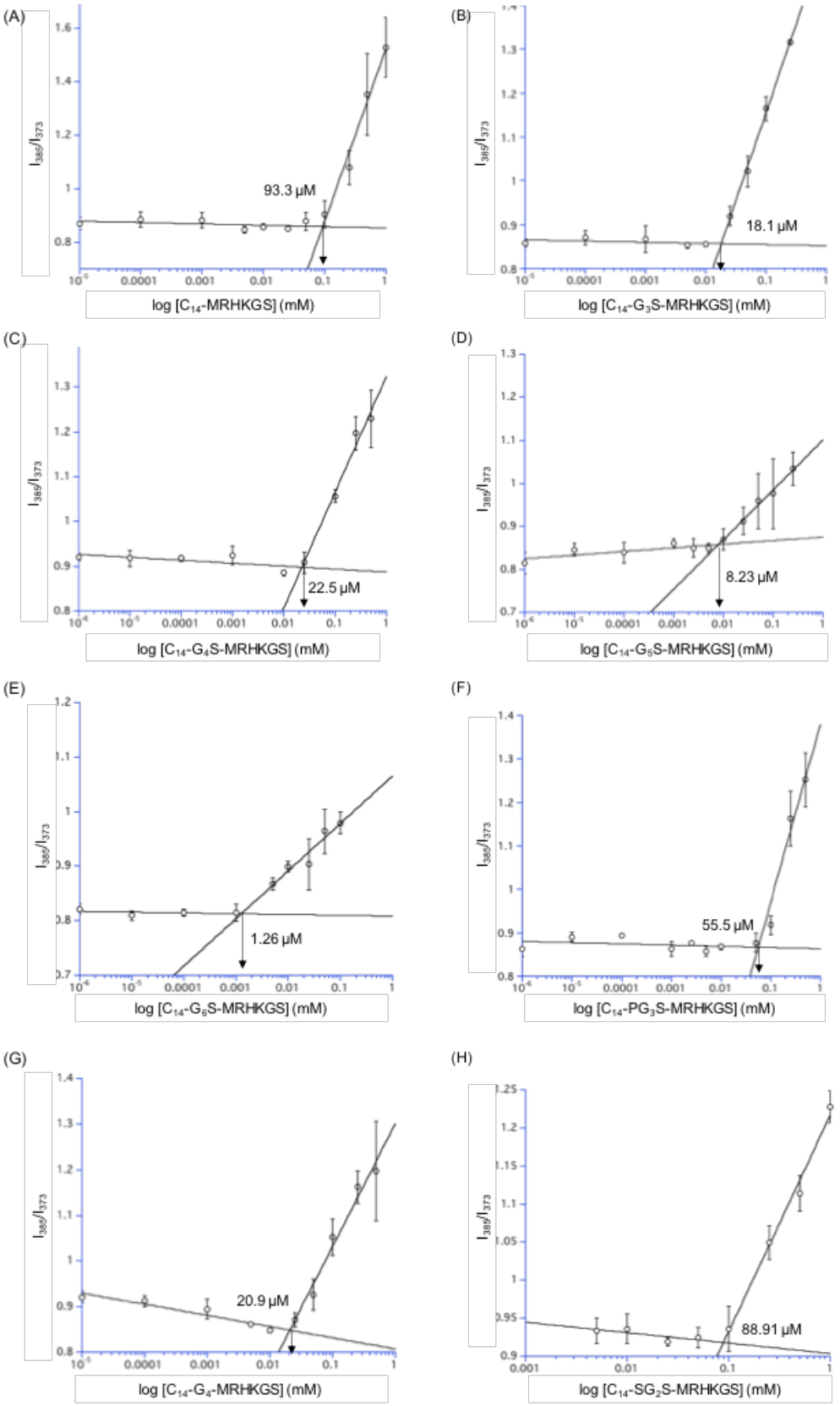

Figure S11. CMC plots of C_{14}-X-MRHKGS. (A) C_{14}-MRHKGS, (B) C_{14}-G_3S-MRHKGS, (C) C_{14}-G_4S-MRHKGS, (D) C_{14}-G_5S-MRHKGS, (E) C_{14}-G_6S-MRHKGS, (F) C_{14}-G_4-MRHKGS, (G) C_{14}- PG_3S-MRHKGS, (H) C_{14}-SG_2S-MRHKGS. Bars represent the standard deviations.

2-8. Cell viability assay of C_{14}-X-MRHKGS

SNU-1 cells suspended in 25 µL Opti-MEM (Thermo Fisher Scientific) were seeded at a concentration of 1.0×10^4 cells/well in a clear 96-well tissue culture plate. Subsequently, C_{14}-X-MRHKGS peptides (0-500 µM/well) dissolved in 25 µL Opti-MEM were added to cells, followed by 24-hour incubation at 37°C with 5% CO_2. The incubation was performed using three parallel samples. After incubation, the viability of SNU-1 cells was determined using Cell Counting Kit-8 (Dojindo Laboratories, Kumamoto, Japan) according to the manufacture's protocol. The absorbance of WST-8 at 450 nm was measured by microplate reader. The cell viability was determined using following equation:

Cell viability (%) = $\{OD_{450}$ (sample) − OD_{450} (blank)$\}$ ×100/ $\{OD_{450}$ (non-treatment) − OD_{450} (blank)$\}$; blank means Opti-MEM and WST-8 alone without cells. The absorbance was measured for three parallel samples.

The cell viability of each C_{14}-X-MRHKGS peptides was plotted against concentration of them. The 50% cytotoxicity concentration (CC_{50}) for each peptide were calculated from the fitted sigmoidal curves generated by KaleidaGraph (Synergy Software, Reading, PA).

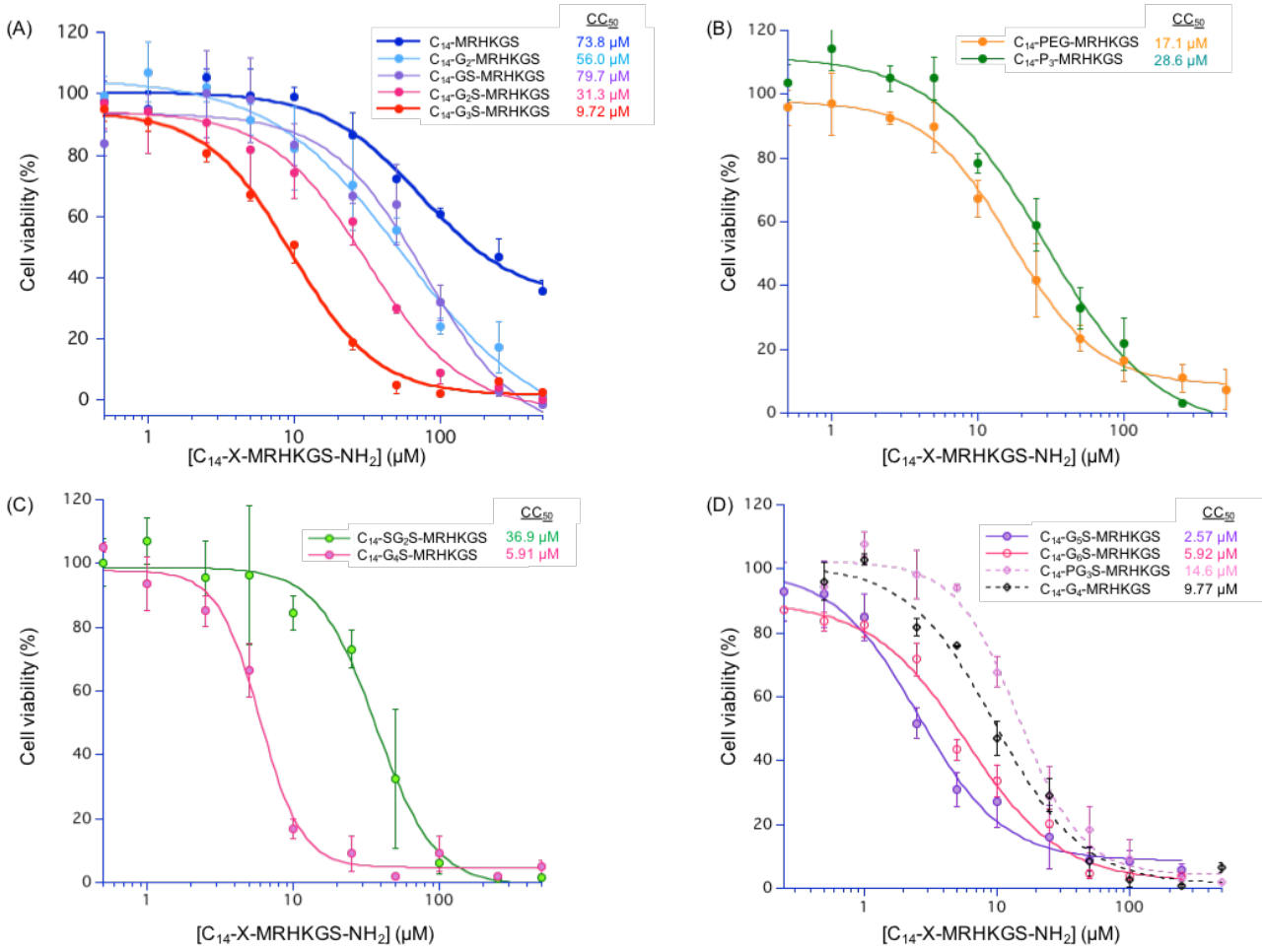

Figure S12. Cell viability assays of C_{14}-X-MRHKGS. (A) C_{14}-MRHKGS, C_{14}-G_nS-MRHKGS (n = 1-3), C_{14}-G_2-MRHKGS, (B) C_{14}-PEG-MRHKGS, C_{14}-PG_3-MRHKGS, (C) C_{14}-SG_2S-MRHKGS, C_{14}-G_4S-MRHKGS, (D) C_{14}-PG_3S-MRHKGS, C_{14}-G_4-MRHKGS, C_{14}-G_nS-MRHKGS (n = 5, 6). Bars represent the standard deviations.

2-9. Dynamic light scattering (DLS) measurement of C_{14}-X-EGFP

MTG reaction product (10 μM LQ-EGFP, 50 μM C_{14}-X-MRHKGS, 0.1 U/mL MTG for 30 min, stopped by 1 mM NEM) was diluted to 1 μM lipidated-EGFP in PBS. The particle size of LQ-EGFP or C_{14}-X-EGFP was measured by dynamic light scattering (DLS) using a Zetasizer Nano ZS (Malvern, Worcestershire, UK.). The DLS results were shown in Figure S13. In Figure S13, C_{14}-EGFP, C_{14}-PG_3S-EGFP, C_{14}-G_6S-EGFP showed almost the same diameter as LQ-EGFP alone, while C_{14}-G_3S-EGFP, C_{14}-G_4S-EGFP, C_{14}-G_5S-EGFP showed larger diameter than that of EGFP alone. This result indicates that C_{14}-G_nS-EGFP (n = 3-5) whose secondary structure of peptides is β-sheet formed co-assembled micelle composed of C_{14}-G_nS-EGFP and unreacted C_{14}-G_nS-MRHKGS. Also, after purification of C_{14}-G_5S-EGFP, the diameter of purified C_{14}-G_nS-EGFP increased from that before purification, indicating that unreacted C_{14}-G_5S-MRHKGS supports the compact micelle formation.

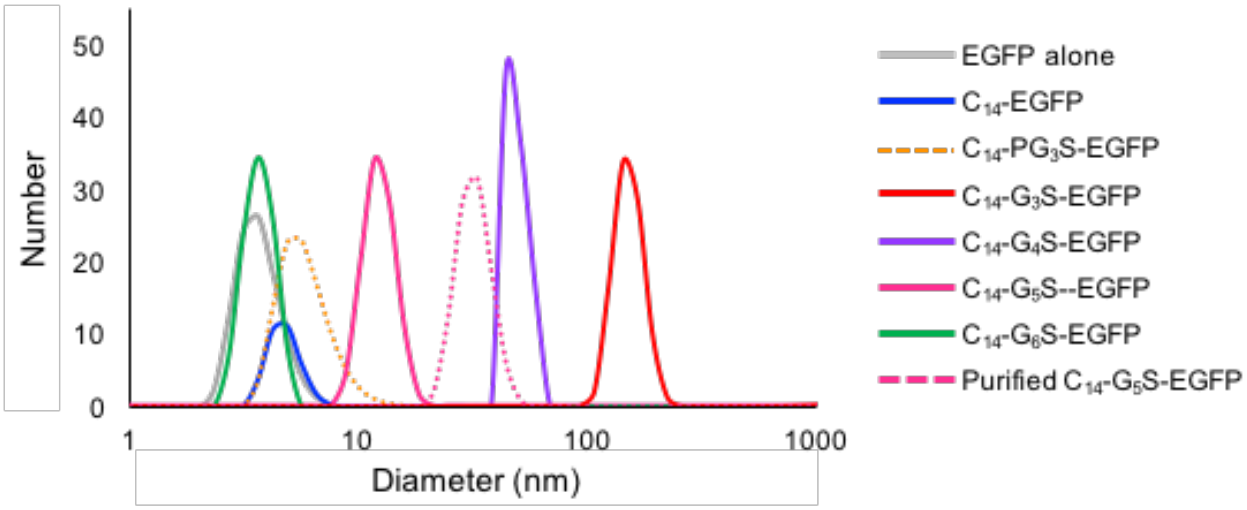

Figure S13. DLS results of C_{14}-EGFP, C_{14}-PG_3S-EGFP and C_{14}-G_nS-MRHKGS (n = 3-6).

2-10. Flowcytometry of C_{14}-G_nS-EGFP

The time-course and concentrations of C_{14}-G_nS-EGFP (n = 3-5) anchoring on a cell membrane of SNU-1 were assessed. In Figure S15 (A), interaction of C_{14}-G_3S-EGFP (5 μM) and SNU-1 was saturated at 15 min, and slightly decreased fluorescence was observed after 30 min incubation. The decreased fluorescence was assumed to be the incorporation of C_{14}-G_3S-EGFP into the intracellular domain,[1] resulting in apparent weaken fluorescence inside the SNU-1 cell. The concentration dependence of C_{14}-G_nS-EGFP incubated with SNU-1 for 15 min was shown in Figure S15 (B). The fluoresce per a cell showed maximum intensity at 5 μM C_{14}-G_nS-EGFP, and linearity was appeared in the range from 0.5 μM to 5 μM of C_{14}-G_nS-EGFP. Thus, we employed the condition of 5 μM C_{14}-X-EGFP incubation with SNU-1 cells for 15 min as an evaluation for membrane-anchoring ability of C_{14}-X-EGFP.

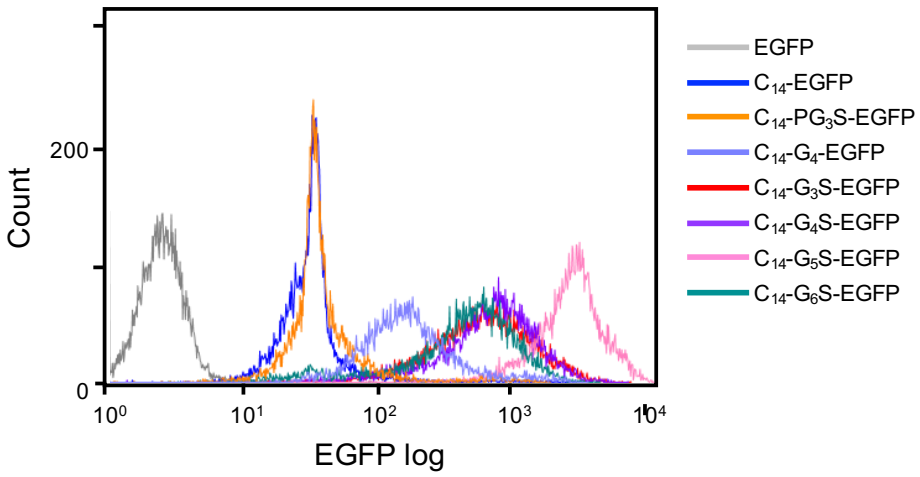

Figure S14. The flowcytometry histogram of Figure 4.

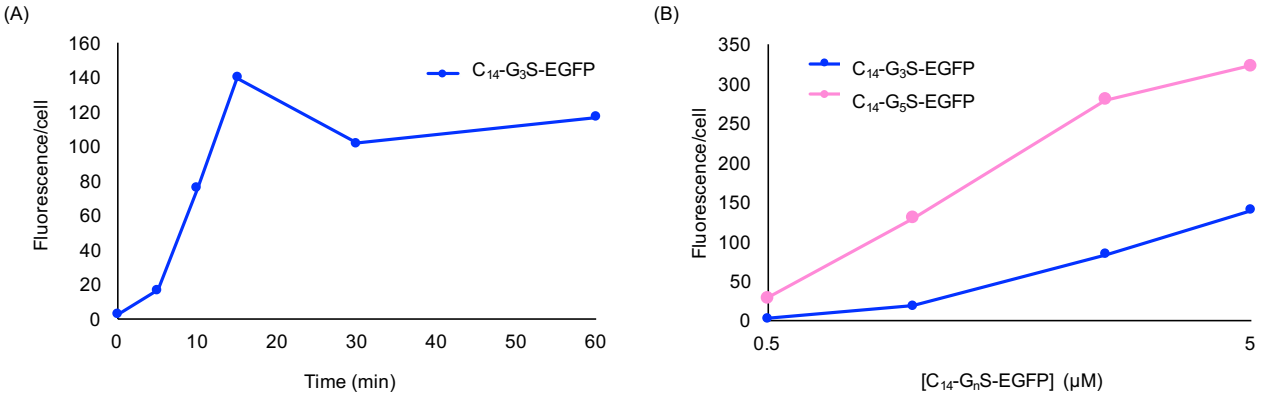

Figure S15. Flowcytometry results of 5 μM C_{14}-G_nS-EGFP (n = 3 or 5) with SNU-1 cells for (A) time-course analysis and (B) concentration dependence of membrane-anchoring.

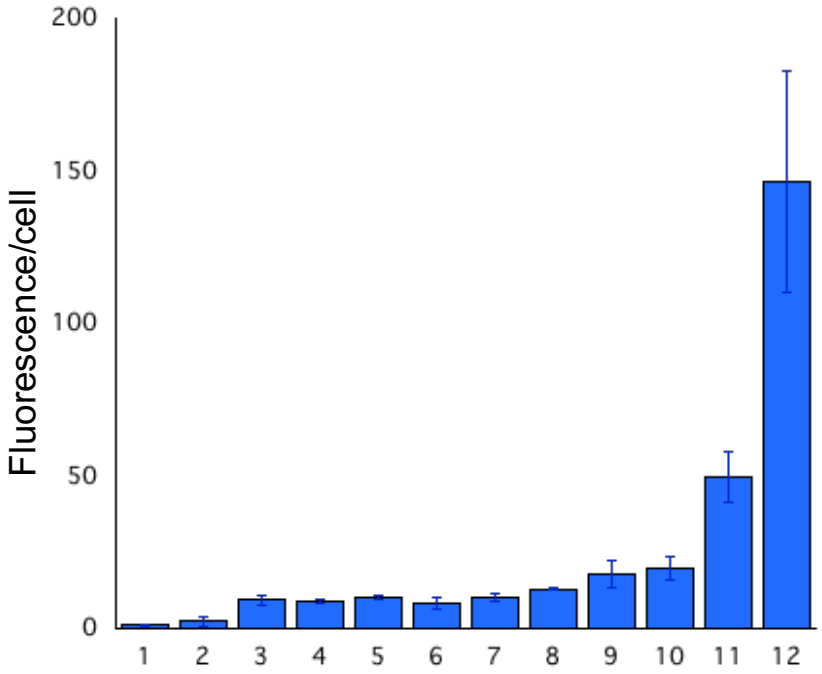

Figure S16. Flowcytometry results of 5 μM C_{14}-X-EGFP with SNU-1 cells. 1) Non-treatment, 2) LQ-EGFP alone, 3) C_{14}-EGFP, 4) C_{14}-PEG-EGFP, 5) C_{14}-PG_3-EGFP, 6) C_{14}-G_2-EGFP, 7) C_{14}-GS-EGFP, 8) C_{14}-G_2S-EGFP, 9) C_{14}-SG_2S-EGFP, 10) C_{14}-PG_3S-EGFP, 11) C_{14}-G_4-EGFP, 12) C_{14}-G_3S-EGFP. Bars represent the standard deviations.

2-11. Cell viability assay of MTG reaction products

The 5.0×10^4 cells/well of SNU-1 suspended in D-PBS (25 µL) were harvested in a 96-well plate. The MTG reaction product containing 10 µM C_{14}-X-EGFP was added to each well in a total volume of 50 µL (1 or 5 µM/well C_{14}-X-EGFP, 5 or 25 µM C_{14}-X-MRHKGS). After incubation for 15 min, MTG reaction solutions were removed. The cells were rinsed twice using D-PBS (100 µL/well) and subsequently subjected to WST-8 reagent (Dojindo, Kumamoto, Japan) in order to determine the viability of the cells. After 90 min incubation, the absorbance at 450 nm (OD_{450}) of WST-8 formazan was measured and cell viability was calculated using following equation:

Cell viability (%) = {OD_{450} (sample) − OD_{450} (blank)} ×100/ {OD_{450} (non-treatment) − OD_{450} (blank)}; blank means Opti-MEM and WST-8 alone without cells. The absorbance was measured for three parallel samples.

The relative cell viability was shown in Figure S17. The cytotoxicity was shown for 5 µM C_{14}-X-EGFP and 25 µM C_{14}-X-MRHKGS mixture since the concentration of C_{14}-X-MRHKGS was higher than CC_{50} except for C_{14}-MRHKGS. In the case of 1 µM C_{14}-X-EGFP and 5 µM C_{14}-X-MRHKGS mixture, where the concentration of C_{14}-X-MRHKGS was under the CC_{50}, there was little cytotoxicity.

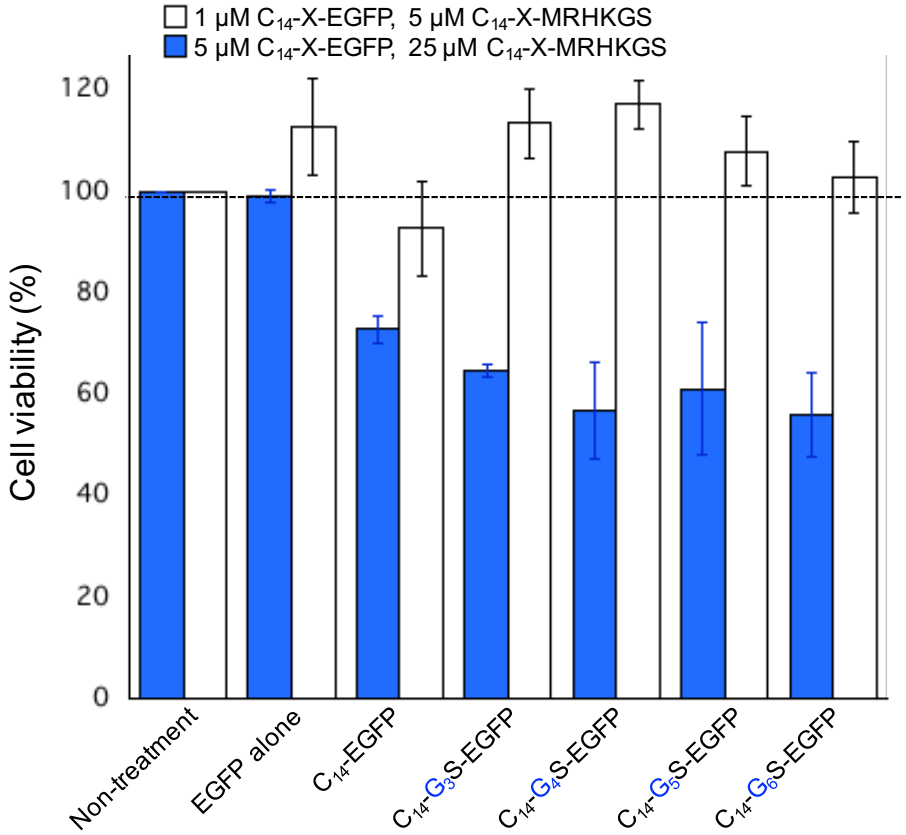

Figure S17. The relative cell viabilities after each C_{14}-X-EGFP incubation. Blue column: 5 µM C_{14}-X-EGFP and 25 µM C_{14}-X-MRHKGS. White column: 1 µM C_{14}-X-EGFP and 5 µM C_{14}-X-MRHKGS. Bars represents the standard deviations.

2-11. Flowcytometry of purified C_{14}-G_5S-EGFP

Flowcytometry results of C_{14}-G_5S-EGFP before or after purification anchored on SNU-1 cells were shown in Figure S18. After purification, C_{14}-G_5S-EGFP showed lower fluorescence per a cell than that of unpurified one, suggesting unreacted C_{14}-G_5S-MRHKGS played some role in interaction among C_{14}-G_5S-EGFP and the cell membrane of SNU-1.

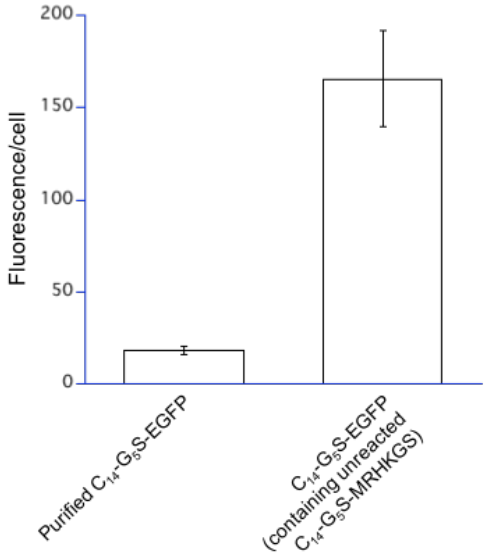

Figure S18. Flowcytometry results of 1 μM C_{14}-G_5S-EGFP with SNU-1 cells before or after purification. Bars represent the standard deviations.

3. References

[1] Antos, J. M.; Miller, G. M.; Grotenbreg, G. M.; Ploegh, H. L., Lipid Modification of Proteins through Sortase-catalyzed Transpeptidation. *J. Am. Chem. Soc.* **2008,** *130*, 16338-16343

[2] Abe, H.; Goto, M.; Kamiya, N., Protein Lipidation Catalyzed by Microbial Transglutaminase. *Chem. - Eur. J.* **2011**, *17*, 14004-14008.

[3] Aguiar, J.; Carpena, P.; Molina-Bolívar, J. A.; Carnero Ruiz, C., On the Determination of the Critical Micelle Concentration by the Pyrene 1:3 ratio method. *J. Colloid Interface Sci.* **2003**, *258*, 116-122.